ACADEMIC PRESS

Available online at www.sciencedirect.com
SCIENCE DIRECT®

Journal of Catalysis 218 (2003) 88–103

JOURNAL OF CATALYSIS

www.elsevier.com/locate/jcat

Reaction kinetics studies and analyses of isobutane conversion over H-mordenite and β-zeolite

Marco A. Sanchez-Castillo,[a] Nitin Agarwal,[a] Andy Bartsch,[a] Randy D. Cortright,[a] Rostam J. Madon,[b] and J.A. Dumesic [a,*]

[a] *Department of Chemical Engineering, University of Wisconsin, Madison, WI 53706, USA*
[b] *Engelhard Corporation, 101 Wood Avenue, Iselin, NJ 08830, USA*

Received 17 October 2002; revised 30 January 2003; accepted 5 February 2003

Abstract

Reaction kinetics data were collected for the conversion of isobutane over H-mordenite and β-zeolite, under conditions where reaction was initiated primarily by addition of isobutylene to the feed and where stable catalyst performance was achieved. We successfully extended our kinetic model, previously developed to describe the conversion of isobutane over USY, to describe the reaction kinetics data of the present study. Catalyst performance for isobutane conversion is controlled primarily by composite activation energies, defined in terms of the energies of transition states relative to gas-phase reactants. The composite activation energies of monomolecular activation steps are lower by about 20–25 kJ mol^{-1} over H-mordenite and β-zeolite compared to USY. In addition, the composite activation energies for hydride transfer and oligomerization/β-scission steps are lower by about 20–30 kJ mol^{-1} over H-mordenite and β-zeolite compared to USY. This result suggests that the same zeolitic interactions responsible for stabilizing the transition states for monomolecular activation are also important for stabilizing the transition states for hydride transfer and oligomerization/β-scission reactions. Our results also suggest that the heats of adsorption of olefins are more exothermic on H-mordenite and β-zeolite compared to USY, again implying that the same interactions responsible for stabilizing the transition states for monomolecular and bimolecular reactions are also important in stabilizing adsorbed reaction intermediates.

Keywords: Isobutane conversion; USY; H-Mordenite; β-Zeolite; Reaction kinetic studies

1. Introduction

Studies of reactivity trends exhibited by hydrocarbons on solid acid catalysts have contributed significantly to understanding factors that control catalytic activity and selectivity during catalytic cracking [1–24]. Among the different probe reactions that have been studied, the conversion of isobutane is particularly useful because the product distribution provides information about the relative contributions of monomolecular and bimolecular reaction pathways observed during the cracking of light paraffins [25–28]. Recently, we developed a kinetic model to describe the reaction kinetics of isobutane conversion over a USY catalyst for a wide range of reaction conditions [29]. This model described a complex product distribution in terms of a limited number of kinetic parameters and used reaction steps from various families of reactions involved in the cracking process: adsorption/desorption of olefins and paraffins, oligomerization/β-scission, isomerization, hydride transfer, and monomolecular activation or initiation reactions. The model allowed us to obtain composite activation barriers for kinetically significant steps and to perform sensitivity analyses to probe the degree of rate control for all steps in the model [29]. In the present paper, we report reaction kinetics data for the conversion of isobutane over H-mordenite and β-zeolite. While these zeolites are not used commercially for catalytic cracking, various studies in the literature have compared the catalytic properties of these zeolites with USY for monomolecular cracking, with the aim of elucidating the factors that control catalyst performance. Accordingly, we have conducted our study of isobutane conversion over H-mordenite and β-zeolite to determine how the rates of monomolecular activation, oligomerization/

* Corresponding author.
E-mail address: dumesic@engr.wisc.edu (J.A. Dumesic).

0021-9517/03/$ – see front matter
doi:10.1016/S0021-9517(03)00061-7

β-scission, and hydride transfer reactions over these zeolites compare to those over USY.

Various researchers [18,20,24,30] have studied monomolecular activation of light alkanes at elevated temperatures over USY, H-mordenite, and β-zeolite and have shown that catalytic activity may be related to the nature of the pore and its size [20,22,31]. In the present study, we have carried out isobutane conversion at temperatures $\leqslant$ 573 K, where the reaction is initiated primarily by the addition of isobutylene to the alkane feed. Accordingly, these data provide information about the rates of oligomerization/β-scission and hydride transfer, thereby permitting us to determine the extent to which pore size and type, that are known to control monomolecular activation, affect the rates of bimolecular reactions. As before [29,32], we also conduct sensitivity analyses with respect to rate constants for monomolecular and bimolecular reactions to show the degree to which certain relationships control catalyst performance under different reaction conditions.

2. Experimental

Table 1 shows the properties of the H-mordenite and β-zeolite catalysts used in this study. The Brønsted and Lewis acidity were determined by Fourier transform infrared spectroscopy with pyridine as the probe molecule. The FTIR experiments were carried out with a Perkin-Elmer 1750 spectrometer operating in the diffuse reflectance mode, using a Spectra Tech controlled-environment cell, as described elsewhere [33]. The numbers of Brønsted acid sites for β-zeolite and H-mordenite are similar and are lower than those for the USY sample used in our earlier study [29]. The number of Lewis acid sites for β-zeolite is significantly higher than that of the USY catalyst, whereas no Lewis acid sites were detected for H-mordenite.

We carried out our experiments using a combination of two quartz flow reactors connected in series, according to the procedure described in our study with USY [29]. The feed to the first reactor consisted of different fractions of isobutane (AGA, research grade, 99.99%) hydrogen (Praxair, 99% purity), and helium (Praxair, 99% purity) at a total pressure of 1 atm. Hydrogen was purified via a Deoxo Unit (Engelhard) followed by a bed of molecular sieve at 77 K, helium was purified by an activated molecular sieve bed at 77 K, while isobutane, with a total hydrocarbon impurity level below 20 ppm, was used without further purification. The total flow rate of feed to the reactor was 60 cm^3(NTP)/min. We adjusted the temperature of the first reactor, loaded with 1.0 g of a Pt–Sn/L-zeolite catalyst, between 473 and 573 K to vary the dehydrogenation–hydrogenation equilibrium of the isobutane/H_2 gas mixture, and thus control the isobutylene concentration of the feed to the second reactor. The second reactor was loaded with 0.023 g of H-mordenite or 0.022 g of β-zeolite. We diluted both catalysts with 0.057 g of pelleted fumed silica to avoid reactor channeling and, before collecting kinetic data, calcined the catalysts at 773 K for 4 h in dry O_2 at a flow of 200 cm^3(NTP)/min.

Table 1
Physical properties of the zeolite catalysts

Properties	Catalyst		
	USY [a]	H-Mordenite[b]	β-Zeolite[b]
SiO_2/Al_2O_3	3.5[c]	20	25
Total surface area ($m^2\,g^{-1}$)	668	419	563
Unit cell size (Å)	24.549	–	–
Brønsted acid sites ($\mu mol\,g^{-1}$)	662	403	377
Lewis acid sites ($\mu mol\,g^{-1}$)	105	0	498

[a] Ref. [29].
[b] Zeolist International.
[c] $Si/Al_{framework} = 4.8$.

We conducted kinetics measurements over H-mordenite at 523 and 573 K. Feed compositions consisted of 10% hydrogen with 20, 40, or 80% isobutane in helium; we used isobutylene feed levels nominally equal to 50, 100, and 150 ppm. We studied β-zeolite over the temperature range of 473–573 K, using feed compositions of 10% hydrogen with 20 or 80% isobutane in helium, and with isobutylene feed levels nominally equal to 20, 35, 50, 70, and 100 ppm. We analyzed all products in the effluent gas stream with a gas chromatograph (Hewlett-Packard 5890), equipped with a flame ionization detector and a 13-foot Alltech column packed with 80/100 mesh 0.19% picric acid on Graphpac-GC.

3. Results

3.1. Effect of temperature on monomolecular activation

We first evaluated the effects of temperature on the rate of isobutane conversion over H-mordenite and β-zeolite with the temperature of the first reactor maintained at 300 K, where the equilibrium for isobutane dehydrogenation is unfavorable. No isobutylene was detected in the product stream exiting the first reactor, and the feed to the second reactor consisted of only 10% H_2 with 20 or 80% isobutane in helium. We monitored the formation of reaction products from the second reactor while increasing the temperature from 373 K in 25 K intervals.

Over H-mordenite we observed no detectable catalytic activity in the absence of feed olefins at temperatures below 473 K. Activation of isobutane initially detected at 473 K with 80% isobutane in the feed led to the formation of methane, isobutylene, *n*-butane, propane, and isopentane. For experiments conducted with 20% isobutane in the feed, we obtained measurable rates of formation of these products at 573 K. Over β-zeolite we detected products at temperatures above 498 K for isobutane feed concentrations of 20 and 80%. Our results for H-mordenite agree with those reported by Fogash et al. [34], who did not detect activity

for isobutane conversion in the absence of feed olefins on H-mordenite at 473 K. These results in the absence of feed olefins show that isobutane activation becomes measurable at lower temperatures over H-mordenite and β-zeolite compared to over USY where temperatures above 600 K are required [29].

3.2. Product distributions

The main products observed for the conversion of isobutane over H-mordenite and β-zeolite were propane, *n*-butane, and isopentane. We obtained small amounts of *n*-butenes (mostly *trans*-2-butene) under all reaction conditions, and detected only trace amounts of propylene (ca. 5 ppm) for both catalysts. For β-zeolite, we detected propylene only at higher temperatures (523–573 K) and 20% isobutane feed concentration. Additionally, the total amount of heavier hydrocarbons (i.e., species heavier than pentane), when observed, was usually less than 50 ppm for H-mordenite and 10 ppm for β-zeolite. We detected methane over H-mordenite and β-zeolite at 573 K, but did not note any formation of ethane or aromatics under the conditions of this study.

The rate of alkane production over H-mordenite and β-zeolite was similar under the same reaction conditions. No significant effect of isobutane feed concentration was observed for the rate of production of propane and isopentane; however, a slight effect was found for the rate of *n*-butane production over β-zeolite. More importantly, the rate of alkane formation over H-mordenite and β-zeolite was markedly higher than the rate of alkane production previously observed over USY under similar reaction conditions [29]. As an example, Figs. 1a and 1b show the rate of *n*-butane production over USY and β-zeolite at 523 and 573 K, respectively. We report all rates as turnover frequencies (TOF), where we assume the number of active sites to be equal to the number of Brønsted acid sites (Table 1). For experiments conducted with 80% isobutane feed concentration, the rates over H-mordenite and β-zeolite were about 20 to 45 times higher than the rates over USY. As shown in Figs. 1a and 1b, the difference for the rate of *n*-butane production between β-zeolite and USY became even larger for experiments with 20% isobutane feed concentration.

In line with high rates of paraffin production, we found the paraffin/olefin (P/O) ratio to be significantly higher for H-mordenite and β-zeolite compared to that of USY. Figs. 1c and 1d show the P/O ratio for USY and β-zeolite under various reaction conditions. In general, the P/O ratios for β-zeolite were larger than those of USY by about 25 and 10 times, for experiments conducted at 523 and 573 K, respectively. In addition, H-mordenite exhibited a slightly larger P/O ratio than β-zeolite for experiments with 20% isobutane in the feed. Our results agree with those reported by others for the conversion of isobutane over H-mordenite [9,34–36], and HY or USY zeolites [26,27,35,37–42].

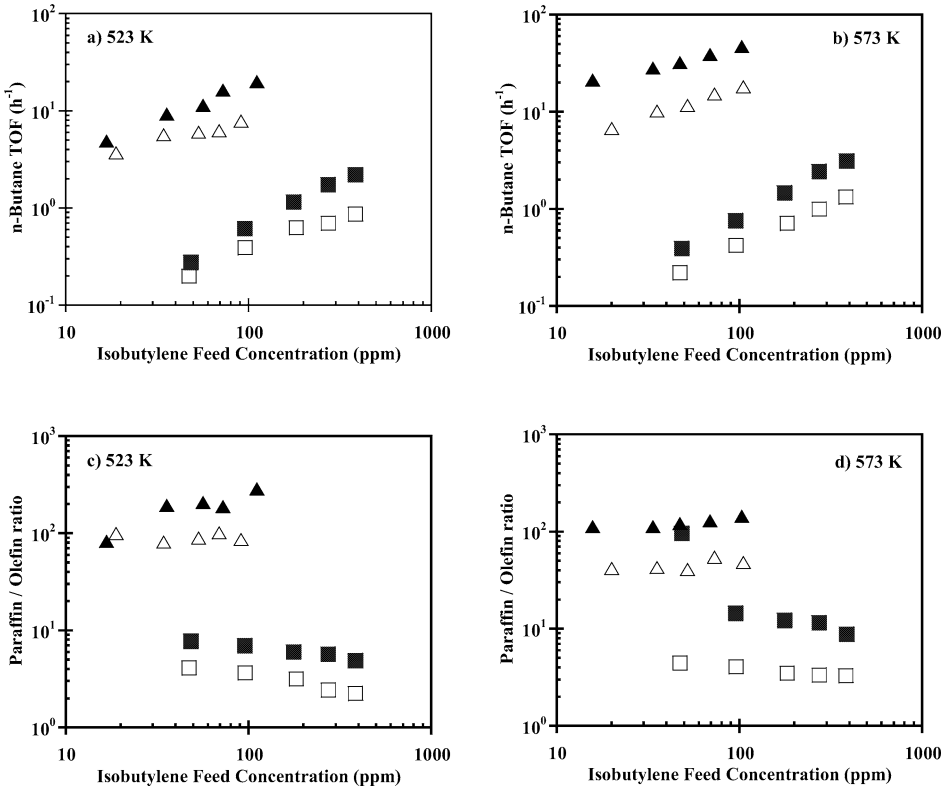

Fig. 1. *n*-Butane TOF and paraffin/olefin ratio as a function of initial isobutylene concentration for USY (squares) and β-zeolite (triangles). Kinetic experiments were conducted with a feed composition of 20% (open symbols) or 80% (full symbols) isobutane, 10% H_2, and He as balance.

3.3. Reaction conditions for stable catalytic performance

Hydrocarbon reactions over solid acid catalysts are typically accompanied by catalyst deactivation over time. We have therefore tried to carry out experiments under conditions where there is little or no observed deactivation. In agreement with our previous kinetic study on USY catalyst [29], and others [39,42], low fractional conversions of isobutane favor stable performance. In the present study we maintained the fractional isobutane conversion below 1%. Fig. 2 shows the rates of paraffin production, as evidenced by the formation of *n*-butane, as a function of time on stream over H-mordenite. Typically, the outlet concentration of isobutylene in the effluent gas and the rates of paraffin production reached steady state after 30 min, and catalyst performance remained stable thereafter for at least 150 min. Fig. 2a shows that at low temperature (523 K) and low isobutane feed concentration (20%), a higher isobutylene concentration led to a more significant decrease in the catalytic activity of H-mordenite with time on stream. However, Fig. 2b shows that this initial decrease in activity was less pronounced at higher isobutane feed concentrations. We believe that the stabilizing effect of isobutane is due to the increase in the rate of hydride transfer reactions over oligomerization reactions, and consequently a decrease in the surface coverage of precursor coke species. For most of the reaction conditions used for H-mordenite, the steady-state concentration of isobutylene in the effluent was equal to about 30–40% of the isobutylene feed concentration. The extent of isobutylene consumption decreased at higher temperature (573 K), and it was practically not affected by isobutane feed concentration. In addition, the extent of isobutylene consumption over H-mordenite at low temperature (523 K) and low isobutylene feed level (below 100 ppm) was higher than that previously observed for USY under similar reaction conditions [29].

Fig. 3 shows, as an example, the rate of *n*-butane production as a function of time on stream over β-zeolite. At high temperatures (573 K), β-zeolite showed negligible deactivation even with 20% isobutane in the feed, irrespective of isobutylene feed concentration. Fig. 3a illustrates the fact that lower temperatures (523 K and below) required an induction time to reach steady activity for all isobutylene feed concentrations. In this case, a high concentration of isobutane in the feed (80%) favored more stable production of *n*-butane. As with H-mordenite, we noted significant consumption of isobutylene under most reaction conditions on β-zeolite.

In summary, we identified conditions where isobutane conversion over H-mordenite and β-zeolite is initiated primarily by feed olefins and where steady-state data may be collected in the absence of deactivation. For H-mordenite, we collected steady-state data at 523 and 573 K, with isobutane feed concentrations of 20, 40, and 80%, and for isobutylene feed concentrations from 50 to 150 ppm. For β-

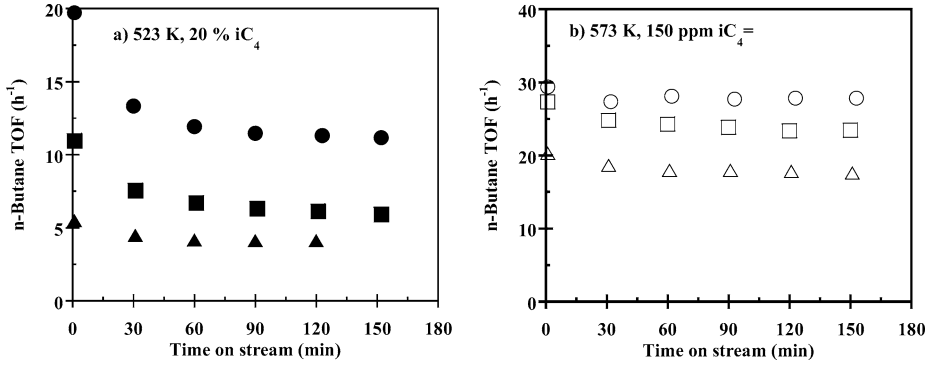

Fig. 2. *n*-Butane TOF as a function of time on stream for kinetic studies conducted over H-mordenite. (a) Feed included: 50 (▲), 100 (■), or 150 (●) ppm of isobutylene; (b) feed included: 20 (△), 40 (□), or 80% (○) isobutane. In all experiments, 10% of H_2 was added and He was used as balance in the feed.

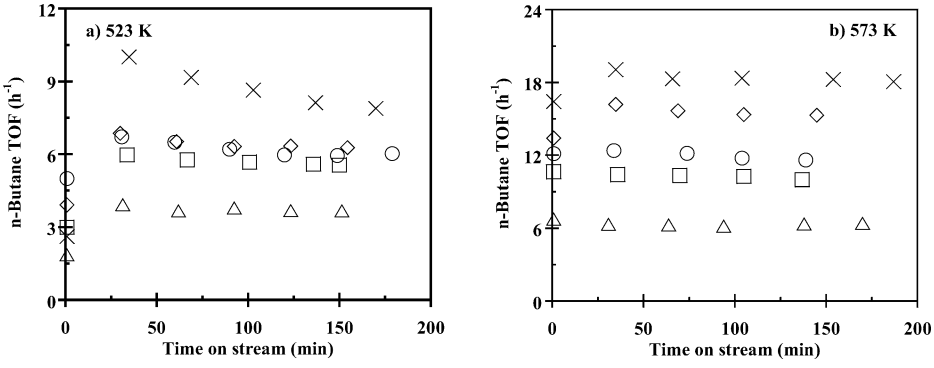

Fig. 3. *n*-Butane TOF as a function of time on stream for kinetic studies conducted over β-zeolite with a feed consisting of 20% isobutane, 10% hydrogen, and isobutylene feed concentration of 20 (△), 35 (□), 50 (○), 70 (◇) and 100 ppm (×). He was used as balance.

zeolite, we collected steady-state data with 20% isobutane feed concentration at 473–573 K, and with 80% isobutane feed concentration at 473–523 K. In each case, we varied the isobutylene feed concentration from 20 to 100 ppm.

3.4. Steady-state rates of formation of alkanes

Over H-mordenite at 523 and 573 K, an increase in isobutylene feed concentration increased the rates of alkane formation for all isobutane feed concentrations (20, 40, and 80%). This effect was more prominent at the higher temperature. For example, at 523 K and 40% isobutane feed concentration, the rate of n-butane production increased from 5.9 to 8.6 h^{-1} when the isobutylene feed level was raised from 50 to 150 ppm. At the same isobutane and isobutylene feed concentrations but 573 K, the corresponding rates of n-butane production increased from 7 to 23.5 h^{-1}. In addition, for a given isobutylene feed level, the rates of alkane formation were essentially independent of the isobutane feed concentration. As an example, the rate of n-butane production at 573 K and 100 ppm of isobutylene feed concentration changed from 18.1 to 16.6 h^{-1}, when the isobutane feed concentration increased from 20 to 80%, respectively. We noted similar trends for the rates of propane and isopentane production.

Over β-zeolite, increasing isobutane feed concentration increased the rates of propane and n-butane production considerably (for isobutylene feed levels higher than 40 ppm), but had a negligible effect on the rate of isopentane formation. For example, at 498 K and 100 ppm of isobutylene feed concentration, the rate of n-butane production increased from 4.5 to 11.6 h^{-1} when the isobutane feed level increased from to 20 to 80%. Conversely, for the same reaction conditions, the rates of isopentane production varied only from 3 to 3.5 h^{-1}. Increasing isobutylene feed concentration led to higher rates of n-butane, propane, and isopentane production for experiments with 80% of isobutane feed concentration for the whole temperature set used in this study. However, for experiments with 20% of isobutane in the feed, the rates of production of all alkanes were markedly increased by the isobutylene feed concentration only at 573 K. At 523 K and below, the rates of n-butane production were almost constant for experiments with more than 40 ppm of isobutylene in the feed.

4. Formulation of the kinetic model

To compare the catalytic properties of H-mordenite and β-zeolite with those of USY, we have analyzed the experimental data obtained in the present study for isobutane conversion over H-mordenite and β-zeolite using the kinetic model that we previously used to describe the kinetics of isobutane conversion over USY [29]. We outline the essential aspects of the kinetic model in this section.

4.1. The reaction scheme

The kinetic model includes steps for monomolecular activation or initiation (we use the terms interchangeably) of isobutane to produce hydrogen or methane and the corresponding alkoxy species [43]. The reaction scheme consists of oligomerization/β-scission, isomerization processes, hydride transfer steps which form paraffins, and desorption of adsorbed alkoxy species to form olefins. Olefin adsorption/desorption steps are reversible, with adsorption steps initiating reactions and desorption steps terminating surface reactions. The reaction scheme for isobutane conversion over H-mordenite and β-zeolite consists of 2 activation steps, 106 oligomerization/β-scission steps, 78 isomerization steps, 88 hydride transfer steps, and 93 adsorption/desorption steps. The reaction scheme includes a total of 190 species, with 93 olefins, 89 surface species, 6 paraffins (with all paraffins having 6 or more carbon atoms grouped as one specie), and hydrogen. We have described in detail elsewhere the procedure to generate this reaction scheme [29].

4.2. Thermodynamic properties

We obtained absolute entropies and enthalpies of formation for gaseous olefins and paraffins in their standard states (i.e., at 1 atm and the reactor temperature) from handbooks for hydrocarbons with fewer than 7 carbon atoms and for heavier hydrocarbons estimated them using Benson's group contribution methods [44–47]. The thermodynamic properties of all surface species are calculated based on standard entropy changes and enthalpy changes of adsorption for gaseous olefins.

We define the enthalpy of formation for a surface species, H_{surface}, in terms of the enthalpy of formation of the corresponding gaseous olefin, H_{olefin}, by

$$H^{\circ}_{\text{surface}} = H^{\circ}_{\text{olefin}} + \Delta H^{\circ}_{3} + \alpha_{\text{H}}(N_{\text{c}} - 3), \tag{1}$$

where $H^{\circ}_{\text{surface}}$ and $H^{\circ}_{\text{olefin}}$ are the enthalpies of formation of the surface species and the corresponding olefin, respectively, ΔH°_{3} is the enthalpy change of adsorption for propylene, N_{c} is the number of carbon atoms in the surface species, and α_{H} is the slope of the linear variation of the adsorption heat with carbon number. We determine ΔH°_{3} from the analysis of the reaction kinetics data. We set α_{H} equal to -0.54 kJ mol^{-1}, the value we used in the USY model [29], because a similar variation of the adsorption heat with carbon number is expected for H-mordenite, β-zeolite, and USY [48,49].

The entropy of formation for a surface species is defined as

$$S_{\text{surface}} = F_{\text{loc}}\left\{\left(S^{\circ}_{\text{gas}} - S_{\text{trans,3D}}\right) + R\ln\left(\frac{2^{n_{\text{surface}}}}{\sigma_{\text{surface}}}\right) - R\ln\left(\frac{2^{n_{\text{gas}}}}{\sigma_{\text{gas}}}\right)\right\}, \tag{2}$$

where S°_{gas} is the absolute entropy of the corresponding gaseous species under the standard state conditions, $S_{\mathrm{trans,3D}}$ is the gaseous translational entropy under these conditions, and n and σ refer to the number of chiral centers and the symmetry numbers of "surface" and "gas" species, respectively. The parameter F_{loc} scales the symmetry-corrected value obtained from the corresponding gas-phase species, and because the adsorbed species involved in the reaction scheme are the same for all catalysts, we set it equal to 1.17, the value obtained from the USY study [29].

4.3. Rate constants

We use the aforementioned thermodynamic values to obtain equilibrium constants for all reactions. Since the equilibrium constant for an elementary step is equal to the ratio of the forward to the reverse rate constants for the step, we can parameterize the model in terms of either rate constant. Table 2 summarizes the rate constants for the various reactions included in the model and indicates the direction of parameterization.

The adsorption/desorption steps are parameterized in the adsorption direction. In our previous study over USY, we found that the activation energy for adsorption, E_{ads}, was kinetically insignificant. Therefore, we use a 30 kJ mol^{-1} value from DFT calculations [50–52] for H-mordenite and β-zeolite so that these steps remain quasiequilibrated.

We calculate the rate constants for the monomolecular activation or initiation steps, k_{init}, using collision theory in the forward direction. Monomolecular activation of isobutane produces hydrogen or methane and the corresponding alkoxy species. Accordingly, we consider two activation energies: $E_{\mathrm{init,H_2}}$ and $E_{\mathrm{init,CH_4}}$. Experimental data for the steady-state concentration of methane, measured for both catalysts under different reaction conditions, allow the evaluation of $E_{\mathrm{init,CH_4}}$ (since methane can only be produced via activation of isobutane). Results of our study with USY show that the activation energies for the two steps of isobutane activation are not very different [29]. Consequently, we constrain both activation energies to the same value.

We parameterize oligomerization/β-scission steps in terms of the β-scission rate constant and set the preexponential factor equal to a typical value of 10^{13} s^{-1}, which corresponds to the entropy of the activated complex being equal to that of the adsorbed reactant species. The activation energy of β-scission, E_{β}, depends on the nature of the β-scission process. We consider three different E_{β} values: $E_{\beta,\mathrm{ss}}$, the activation energy for β-scission of a secondary species to form another secondary species, $E_{\beta,\mathrm{st}}$, corresponding to the β-scission of a secondary species to form a tertiary species or β-scission of a tertiary species to form a secondary species; and $E_{\beta,\mathrm{tt}}$, corresponding to the β-scission of a tertiary species to form another tertiary species. With USY [29], we found the following trend of E_{β} values: $E_{\beta,\mathrm{ss}} = E_{\beta,\mathrm{st}} > E_{\beta,\mathrm{tt}}$.

We found in our previous study with USY [29] under reaction conditions similar to those used here that nonbranching and branching isomerization steps were quasiequilibrated. Accordingly, we set the values of the activation energies for these kinetically insignificant, nonbranching and branching isomerization steps equal to the values we used for USY, 80 and 110 kJ mol^{-1}, respectively, for both H-mordenite and β-zeolite.

We parameterize hydride transfer steps in the direction of the reaction with isobutane. The rate constant includes the activation energy for hydride transfer, E_{H}, and an entropy change related to the formation of the activated complex, $\Delta S^{\dagger}_{\mathrm{Hydride}}$. If $\Delta S^{\dagger}_{\mathrm{Hydride}}$ is equal to zero, then the expression for the rate constant is given by the collision rate of isobutane molecules on the acid sites times the probability that these collisions surmount the activation energy barrier. In view of the narrow temperature range used in the kinetic studies for H-mordenite and β-zeolite, we set $\Delta S^{\dagger}_{\mathrm{Hydride}}$ equal to -24.3 J mol^{-1} K^{-1}, the value obtained from our study with USY [29].

In summary, based on our previous studies of isobutane conversion over USY, we described the reaction kinetics over H-mordenite and β-zeolite using only 6 parameters that are kinetically significant, namely: ΔH_3, E_{β}, $E_{\mathrm{C_3}}$, $E_{\mathrm{C_4}}$, $E_{\mathrm{C_5}}$, and $E_{\mathrm{C_{>5}}}$. We assumed that the reactor operated as a plug-flow reactor and determined the fitted kinetic parameters along with the corresponding 95% confidence interval by using Athena Visual Workbench [53]. Accordingly, we solved 100 differential equations, corresponding to the gaseous molecular flow rates of paraffins (6), olefins (93), and hydrogen versus reactor length. We combined these equations with 89 steady-state equations for the fractional surface coverage by adsorbed species, and 1 site-balance equation.

4.4. Sensitivity analyses

Sensitivity analyses facilitate the identification of kinetically significant steps in a complex multipathway process

Table 2
Definition of the different rate constants for the kinetic model

Step	Parameterization direction	Rate equation
Adsorption/ desorption	Adsorption	$k_{\mathrm{ads}} = \frac{\exp(-\frac{E_{\mathrm{ads}}}{RT})}{\sqrt{2\pi m_{\mathrm{A}} k_{\mathrm{B}} T}} A_{\mathrm{site}}$
Monomolecular activation (initiation)	Reaction with site proton	$k_{\mathrm{init}} = \frac{\exp(-\frac{E_{\mathrm{init}}}{RT})}{\sqrt{2\pi m_{\mathrm{A}} k_{\mathrm{B}} T}} A_{\mathrm{site}}$
Oligomerization/ β-scission	β-Scission	$k_{\beta} = 10^{13} \exp(-\frac{E_{\beta}}{RT})$
Isomerization	Any	$k_{\mathrm{iso}} = 10^{13} \exp(-\frac{E_{\mathrm{iso}}}{RT})$
Hydride transfer	Reaction with isobutane	$k_{\mathrm{H}} = \frac{\exp(\frac{\Delta S^{\ddagger}}{R} - \frac{E_{\mathrm{H}}}{RT})}{\sqrt{2\pi m_{\mathrm{A}} k_{\mathrm{B}} T}} A_{\mathrm{site}}$

k, rate constant; E, activation energy, kJ mol^{-1}; S, entropy, kJ mol^{-1} K^{-1}; R, gas constant; T, temperature; k_{B}, Boltzmann's constant; m_{A}, mass of reactant gas-phase molecule; A, area occupied per site, 10^{-15} cm^2 site^{-1} (typical molecular cross-sectional area).

such as the conversion of isobutane over zeolite catalysts, and thus help determine which reactions control the overall process. In addition, these analyses indicate how the kinetic significance of one step with respect to another changes as a function of reaction conditions. A useful tool to assess kinetically significant steps is Campbell's degree of rate control [54], $X_{\mathrm{RC},i}$, which for step i is defined as

$$X_{\mathrm{RC},i} = \left(\frac{\partial r}{\partial k_{i,\mathrm{for}}}\right)_{K_{\mathrm{eq},i,k_j}} \frac{k_{i,\mathrm{for}}}{r} = \left(\frac{\partial r}{\partial k_{i,\mathrm{rev}}}\right)_{K_{\mathrm{eq},i,k_j}} \frac{k_{i,\mathrm{rev}}}{r}, \quad (3)$$

where each partial derivative represents the change in the overall rate, r, with respect to a change in the forward or the reverse rate constant for step i, $k_{i,\mathrm{for}}$ or $k_{i,\mathrm{rev}}$, keeping the equilibrium constant for step i, $K_{\mathrm{eq},i}$, and all other rate constants k_j constant. In the above expression, the overall rate r is given by the consumption of isobutane. Importantly, the sum of the values of $X_{\mathrm{RC},i}$ for all of the steps is equal to unity for a reaction scheme that leads to a single overall reaction [55]:

$$\sum_i X_{\mathrm{RC},i} = 1. \quad (4)$$

In general, a sum of $X_{\mathrm{RC},i}$ greater than unity indicates the existence of multiple reaction pathways for consumption of the reactant [32]. We note that as conversion approaches 100%, the rate of consumption of the reactant is controlled by the flow rate to the reactor, rather than by values of the rate constants, therefore, the sum of values of $X_{\mathrm{RC},i}$ approaches zero at 100% conversion.

5. Discussion

5.1. Predictions from the kinetic model

Table 3 summarizes values of the kinetic parameters used to describe the reaction kinetics data with H-mordenite and β-zeolite, including 95% confidence intervals for the kinetically significant parameters and compares them with those found previously with USY [29]. Importantly, we find only six parameters to be kinetically significant for H-mordenite and β-zeolite, and the other kinetic parameters are therefore fixed at constant values.

Values of ΔH_3 for H-mordenite and β-zeolite are similar, indicating that the heat of adsorption of alkenes on both catalysts is nearly the same; ΔH_3 for H-mordenite and β-zeolite is more exothermic by 31.2 and 32 kJ mol^{-1}, respectively, compared to that for USY. Since surface coverage on USY was very low under all reaction conditions ($< 1\%$), ΔH_3 for this catalyst was kinetically insignificant and was fixed at a reasonable value of -90 kJ mol^{-1}, as explained in Ref. [29], with the remaining kinetic parameters adjusted to fit the data. However, the kinetic model predicts higher surface coverages by hydrocarbon species on H-mordenite (5 to 52%) and β-zeolite (9 to 63%) under the same reaction conditions used for USY. Therefore, the value of ΔH_3 may be estimated from the reaction kinetics data. At 523–573 K, the most abundant surface species over H-mordenite is the *n*-butyl species for 20% isobutane feed concentration, and the isobutyl species for 80% isobutane. Other species with significant surface concentration at both isobutane feed levels are propyl and isopentyl species. In addition, the fraction of H-mordenite surface covered by heavier adsorbed species is negligible (below 10^{-3}). Results on β-zeolite are similar, with slightly higher adsorbed species fractions than H-mordenite at 523 K.

Table 3
Values of the kinetic parameters for isobutane conversion over various zeolites

Parameter	USY*	H-MOR	β
α_{H}	-0.54	-0.54[a]	-0.54[a]
F_{loc}	1.17 ± 0.01	1.17 [a]	1.17[a]
ΔH_3	-90.0[d]	-121.2 ± 0.9	-122.2 ± 0.5
$E_{\mathrm{init,H_2}}$	156.5 ± 0.5	134.5[b]	129.5[b]
$E_{\mathrm{init,CH_4}}$	154.3 ± 0.5	134.5[c]	129.5[c]
$E_{\beta,\mathrm{tt}}$	102.2 ± 5.8	120.1 ± 0.7	119.2 ± 0.4
$E_{\beta,\mathrm{st}}$	115.1 ± 5.7	120.1 ± 0.7	119.2 ± 0.4
$E_{\beta,\mathrm{ss}}$	115.1 ± 5.7	123.1 ± 3.2	119.2 ± 0.4
$E_{\mathrm{C_3}}$	64.3 ± 1.4	77.4 ± 1.2	78.5 ± 0.5
$E_{\mathrm{C_4}}$	76.5 ± 1.4	82.8 ± 0.7	84.7 ± 0.3
$E_{\mathrm{C_5}}$	62.2 ± 1.7	70.0[d]	75.0 ± 1.0
$E_{\mathrm{C_{\geq 5}}}$	62.2 ± 1.4	72.1 ± 2.1	71.5 ± 0.6
$\Delta S^{\ddagger}_{\mathrm{Hydride}}$	-24.3 ± 2.2	-24.3[a]	-24.3[a]

Activation energies and α_{H} are given in kJ mol^{-1}, entropy changes in J mol^{-1} K^{-1}, and F_{loc} is dimensionless. 95% confidence interval is indicated next to the parameter value.

* Values from Ref. [29].

[a] Value constrained to that for USY.

[b] Value constrained to that of $E_{\mathrm{init,CH_4}}$.

[c] Value constrained to match methane concentration in effluent.

[d] Not kinetically significant.

Table 3 shows that the activation energies for monomolecular activation of isobutane are equal to 129.5 kJ mol^{-1} for β-zeolite and 134.5 kJ mol^{-1} for H-mordenite; and these values are lower that those for USY [29]. Monomolecular activation of isobutane becomes relevant at a lower temperature for β-zeolite (498 K for 20 and 80% isobutane in the feed), and H-mordenite (473 K for 20% or 573 K for 80% isobutane), as compared to USY (> 600 K for both isobutane feed concentrations).

The values of $E_{\beta,\mathrm{ss}}$, $E_{\beta,\mathrm{st}}$ and $E_{\beta,\mathrm{tt}}$ are similar for H-mordenite and β-zeolite, and are higher than those for USY. However, the values of E_β for USY are linked to the kinetically insignificant values of ΔH_3. Therefore, comparison of the values of E_β will be discussed later in terms of composite activation energies, where we include the value of ΔH_3.

The trends in the various activation energies for hydride transfer steps over H-mordenite and β-zeolite are similar to those for USY; $E_{\mathrm{C_4}}$ in each case is the highest. We found the value of $E_{\mathrm{C_5}}$ over H-mordenite to be kinetically insignificant and fixed it at 70 kJmol^{-1}, the value at which it becomes kinetically significant (that is, the value above which it affects the prediction of the kinetic model). Activation

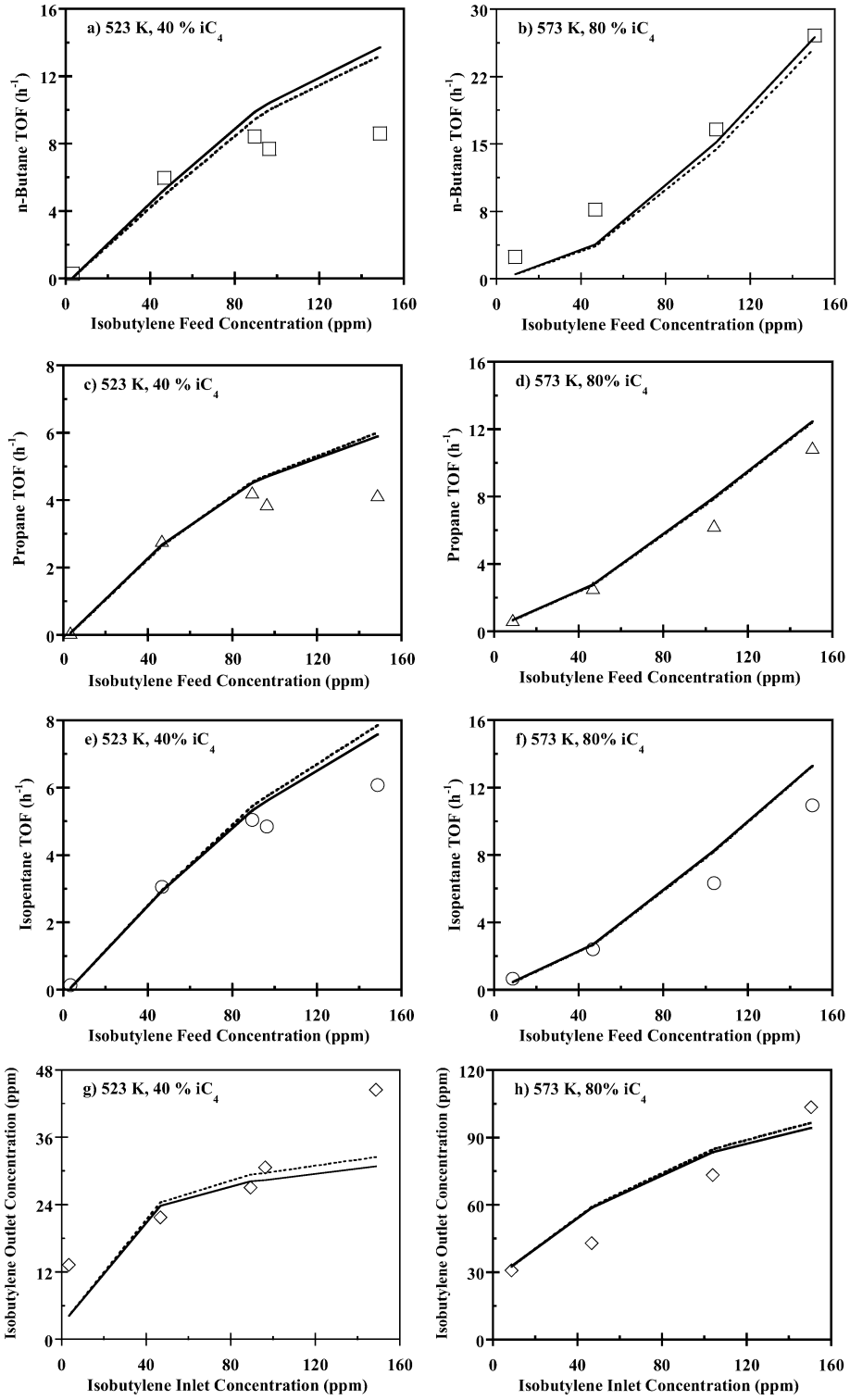

Fig. 4. Paraffin TOFs and isobutylene outlet concentration over H-mordenite as a function of isobutylene feed concentration. (a and b) *n*-Butane, (c and d) propane, (e and f) isopentane, and (g and h) isobutylene. Predictions of the kinetic model are given by solid lines for the full model and dotted lines for the simplified model.

energies for hydride transfer over β-zeolite are closer to those for H-mordenite, and in both cases are larger than those for USY by more than ca. 10 kJ mol^{-1}.

The solid lines in Fig. 4 show the predictions of the kinetic model for the rates of formation of propane, *n*-butane, and isopentane, as well as the outlet concentration of isobutylene, over H-mordenite for various reaction conditions. In general, the kinetic model describes the experimental trends for all the paraffins. The kinetic model begins to underpredict the rates of paraffin production at lower isobu-

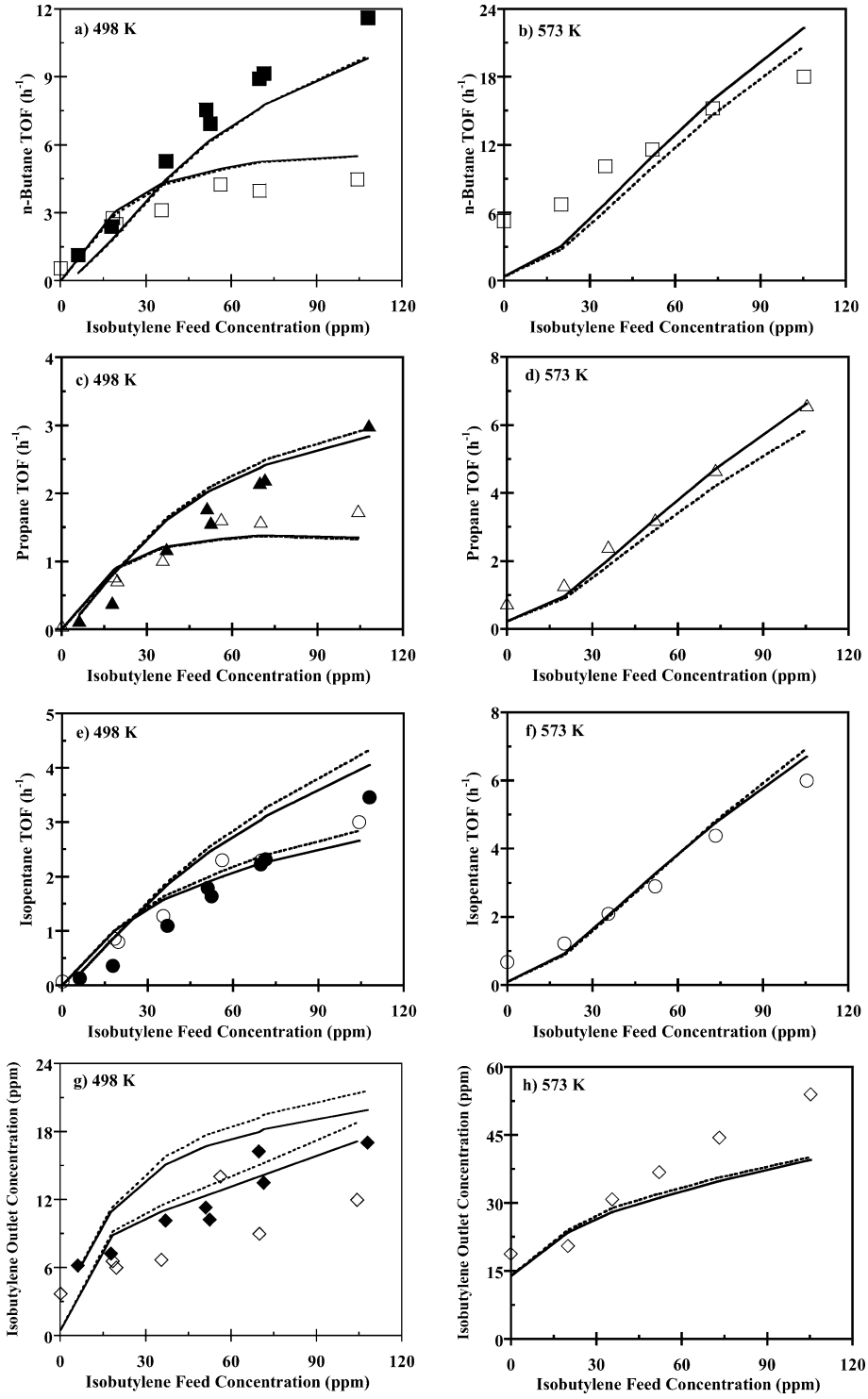

Fig. 5. Paraffin TOFs and isobutylene outlet concentration over β-zeolite as a function of isobutylene feed concentration. (a and b) *n*-Butane, (c and d) propane, (e and f) isopentane, and (g and h) isobutylene. The experiments were conducted with a feed composition of 20% (open symbols) or 80% (full symbols) isobutane, 10% H_2, and He as balance. Predictions of the kinetic model are given by solid lines for the full model and dotted lines for the simplified model.

tane feed concentrations (i.e., below 40%) and high isobutylene feed levels (i.e., above 100 ppm), particularly at low temperature (i.e., 523 K and below). These conditions lead to high surface coverages by adsorbed species, and these data are not shown in Fig. 4.

The predictions of the kinetic model for isobutane conversion over β-zeolite are shown as solid lines in Fig. 5 for the rates of formation of propane, *n*-butane, and isopentane, as well as the outlet concentration of isobutylene, under various reaction conditions. The kinetic model describes the exper-

imental trends for all the paraffins and isobutylene for most of the reaction conditions. We find deviations from experimental data only at low temperature and high isobutane and isobutylene feed concentrations. For instance, at 473 K and 100 ppm of isobutylene in the feed a difference of about 40% between the observed and the predicted *n*-butane TOF is found for experiments conducted with 80% isobutane in the feed. Predictions of the model at this low temperature indicate that the surface of β-zeolite is highly covered by adsorbed species. We suggest that the kinetic model may become unreliable at these high coverages ($> 70\%$).

5.2. Comparison of H-mordenite and β-zeolite with USY

Various groups have compared activation energies for monomolecular activation of light alkanes over acidic zeolite catalysts [3,30,31]. These comparisons use the composite activation energy (E_{comp}), which is the sum of the heat of adsorption of the alkane (ΔH_{ads}) and the intrinsic activation energy (E_{intr}), as initially suggested by Haag [3]:

$$E_{\text{comp}} = \Delta H_{\text{ads}} + E_{\text{intr}}. \tag{5}$$

Accordingly, the value of the composite activation energy represents the energy of the transition state for monomolecular activation relative to the gaseous alkane reactant. We recently used this approach to elucidate the differences in activity and selectivity of USY catalysts during the conversion of isobutane and 2-methylhexane [29,32]. We now follow a similar approach to compare the catalytic performance of H-mordenite and β-zeolite with that of USY.

Table 4 shows composite activation energies for the three catalysts. We obtain the composite barriers for the oligomerization/β-scission steps and the hydride transfer steps by adjusting the actual barriers by ΔH_3°, in accord with Eq. (5). These composite activation energies represent the energies of the transition states *relative to gaseous reactants*. Since activation barriers for monomolecular activation of isobutane are already defined with respect to the gas phase, no further adjustment is required for these barriers.

Table 4
Values of composite activation energies. All composite activation energies are given in kJ mol^{-1}

Composite	Catalyst					
energy	USY[a]	H-M	β	Δ(USY,H-M)	Δ(USY,β)	Δ(H-M,β)
$E_{\text{tt}} + \Delta H_3$	12.2	−1.1	−3.0	13.2	15.2	1.9
$E_{\text{st}} + \Delta H_3$	25.1	−1.1	−3.0	26.2	28.1	1.9
$E_{\text{ss}} + \Delta H_3$	25.1	1.9	−3.0	23.2	28.1	4.9
$E_{\text{C}_3} + \Delta H_3$	−25.7	−43.9	−43.7	18.2	18.0	−0.1
$E_{\text{C}_4} + \Delta H_3$	−13.5	−38.4	−37.5	24.9	24.0	−0.9
$E_{\text{C}_5} + \Delta H_3$	−27.8	–	−47.2	–	19.4	–
$E_{\text{C}_{>5}} + \Delta H_3$	−27.8	−49.1	−50.7	21.3	22.9	1.6
$E_{\text{init,H}_2}$	156.5	134.5	129.5	22.0	27.0	5.0
$E_{\text{init,CH}_4}$	154.3	134.5	129.5	19.8	24.8	5.0

Last three columns indicate the difference between the composite activation energy values for USY and H-mordenite, Δ(USY,H-M); USY and β-zeolite, Δ(USY,β); and H-mordenite and β-zeolite, Δ(H-M,β).

[a] From Ref. [29].

Table 4 shows that the activation energies for monomolecular activation of isobutane over H-mordenite are lower than those over USY by about 20 kJ mol^{-1}. This result agrees with previous findings in the literature. For example, Babitz et al. [20] reported a difference of 20 kJ mol^{-1} between the composite activation energies for monomolecular activation of *n*-hexane over H-mordenite and H-USY catalysts. Activation energies for monomolecular activation of isobutane over β-zeolite are lower than those of USY by about 26 kJ mol^{-1}. This result agrees with previous findings of Kotrel et al. [30], who reported a difference of about 21 kJ mol^{-1} between the apparent activation energies for monomolecular activation of hexane over H-β and H-Y zeolite catalysts.

Haag et al. [3] and Narbeshuber et al. [31] have suggested that differences in the composite activation energies for monomolecular activation over zeolites are related to differences in the heats of *n*-alkane adsorption. In concert with this idea, when we compare H-mordenite and β-zeolite to USY, we find that differences of composite activation energies for monomolecular activation of isobutane are in agreement with differences in the heats of alkane adsorption for these zeolites. For example, Denayer et al. [49] reported that the adsorption of *n*-pentane was stronger by 19 kJ mol^{-1} for H-mordenite compared to Y-zeolite, and the heat of *n*-hexane adsorption was stronger by 23 kJ mol^{-1}. Similarly, Kotrel et al. [30] reported that the heat of *n*-hexane adsorption was stronger by 20 kJ mol^{-1} over β-zeolite compared to Y-zeolite.

Fig. 6 further illustrates the comparison of the composite energies for monomolecular activation and propagation steps (i.e., hydride transfer or oligomerization/β-scission) shown in Table 4. As an example, Fig. 6 shows schematic representations of the composite barriers for monomolecular activation of isobutane and the hydride transfer reaction between propyl species and gas-phase isobutane for both, USY (solid lines) and H-mordenite (dotted lines). Fig. 6a shows that the composite energy for monomolecular activation of isobutane over H-mordenite is 19.8 kJ mol^{-1} lower than that of USY. Similarly, Fig. 6b shows that the composite energy (i.e., with respect to gas phase) for the hydride transfer reaction over H-mordenite is 18.2 kJ mol^{-1} lower than that of USY, as indicated in column Δ(USY,H-M) of Table 4. In general, the composite activation energies for oligomerization/β-scission (neglecting E_{tt}) and hydride transfer steps over H-mordenite are generally lower by ca. 20 kJ mol^{-1} compared to those over USY (Table 4). For β-zeolite, the values are generally lower by a range of ca. 20–28 kJ mol^{-1} with respect to those for USY. Thus, the differences of the composite activation energies found for β-scission and hydride transfer are similar to the aforementioned differences in the composite activation energies for monomolecular activation steps. Importantly, *this result suggests that the same interactions responsible for stabilizing*

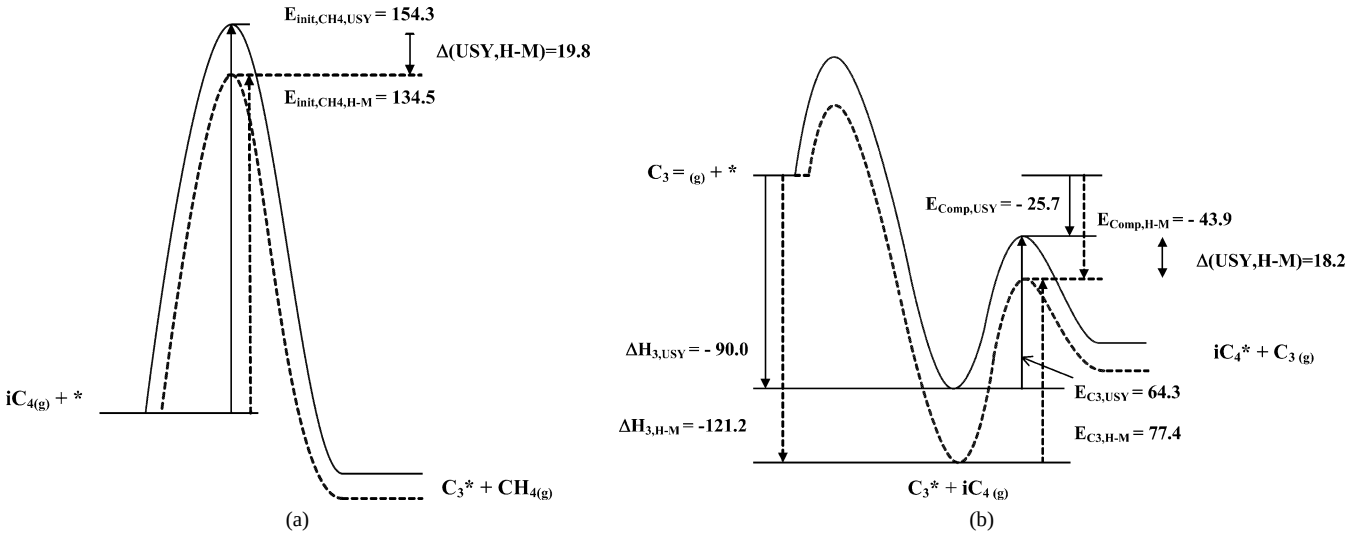

Fig. 6. Schematic diagram for comparison of composite activation energies for USY (full line) and H-mordenite (dotted line): (a) initiation step; (b) hydride transfer of isobutane and C_3* species. Enthalpy of adsorption and all energies values are given in kJ mol^{-1}.

the transition states for monomolecular activation over zeolites are also important in stabilizing the transition states for β-scission and hydride transfer. These interactions are most likely caused by van der Waals and electrostatic forces between the hydrocarbon moieties and the micropore walls of the zeolite.

As noted earlier, the value of ΔH_3 is kinetically insignificant for USY, because surface coverage by adsorbed species is low under all reaction conditions. In contrast, the value of ΔH_3 can be estimated from reaction kinetics measurements over H-mordenite and β-zeolite because these catalysts operate at higher surface coverages. Adsorption of olefins (related to ΔH_3) is more exothermic on H-mordenite and β-zeolite compared to USY. *This result suggests that the same interactions responsible for stabilizing the transition states for monomolecular activation, β-scission, and hydride transfer are also important in stabilizing the adsorbed surface alkoxy reaction intermediates.*

5.3. Sensitivity analyses

Using Eq. (3), we calculated Campbell's degree of rate control, $X_{\mathrm{RC},i}$, for each step in the reaction scheme for H-mordenite and β-zeolite, identified the kinetically significant steps, and thus built a smaller kinetic model by combining these steps with a limited number of quasiequilibrated steps to interconnect quasiequilibrated intermediates. Our results show that the same steps are kinetically significant over both H-mordenite and β-zeolite, although the degree of significance of each step is slightly different for each catalyst. The simplified reaction scheme over H-mordenite and β-zeolite shown in Fig. 7 is similar to the simplified scheme developed for USY [29]. The predictions of this simplified model for each catalyst are indicated by dashed lines in Fig. 4 for H-mordenite and in Fig. 5 for β-zeolite, and agree with the predictions of the full kinetic model. Importantly, no further adjustment of the kinetic parameters was required after the sensitivity analysis. Thus, the same set of kinetic parameters was employed for the extended and the simplified kinetic models.

Fig. 8 shows the sum of the absolute values of Campbell's degree of rate control, $\sum |X_{\mathrm{RC},i}|$, for monomolecular activation, hydride transfer, and β-scission, as a function of isobutylene feed concentration at two different temperatures, 473 and 573 K, and isobutane feed concentrations, 20 and 80%. We conducted these simulations using the same site velocity for all three catalysts (i.e., the same flow rate of isobutane per acid site); therefore, since the composite activation energies for USY are higher, the conversion of isobutane is lower for USY compared to that for H-mordenite and β-zeolite. We also give in Fig. 9 the corresponding steady-state net rates calculated at the exit of the plug flow reactor for monomolecular activation, hydride transfer, and β-scission steps. Results of the sensitivity analysis for β-zeolite at 573 K and 80% isobutane were calculated by extrapolation of the reaction conditions used for the kinetic analysis.

Since trends of $\sum |X_{\mathrm{RC},i}|$ for all three reaction families for H-mordenite are the same as for β-zeolite, we will compare only the latter to results over USY. Fig. 8 shows that trends for each reaction family vary as a function of reaction conditions differently for USY and β-zeolite. For USY, $\sum |X_{\mathrm{RC},i}|$ for monomolecular activation steps is negligible at 473 K, and becomes noticeable only at 573 K and isobutylene feed concentration below 100 ppm. For hydride transfer and β-scission on USY, $\sum |X_{\mathrm{RC},i}|$ depends on isobutane feed concentration. For 20% isobutane concentration, $\sum |X_{\mathrm{RC},i}|$ for hydride transfer steps is higher than for β-scission steps over the whole range of reaction temperatures and isobutylene feed concentrations. For 80% isobutane feed concentration and isobutylene levels between 150 and 200 ppm, the higher degree of rate control shifts

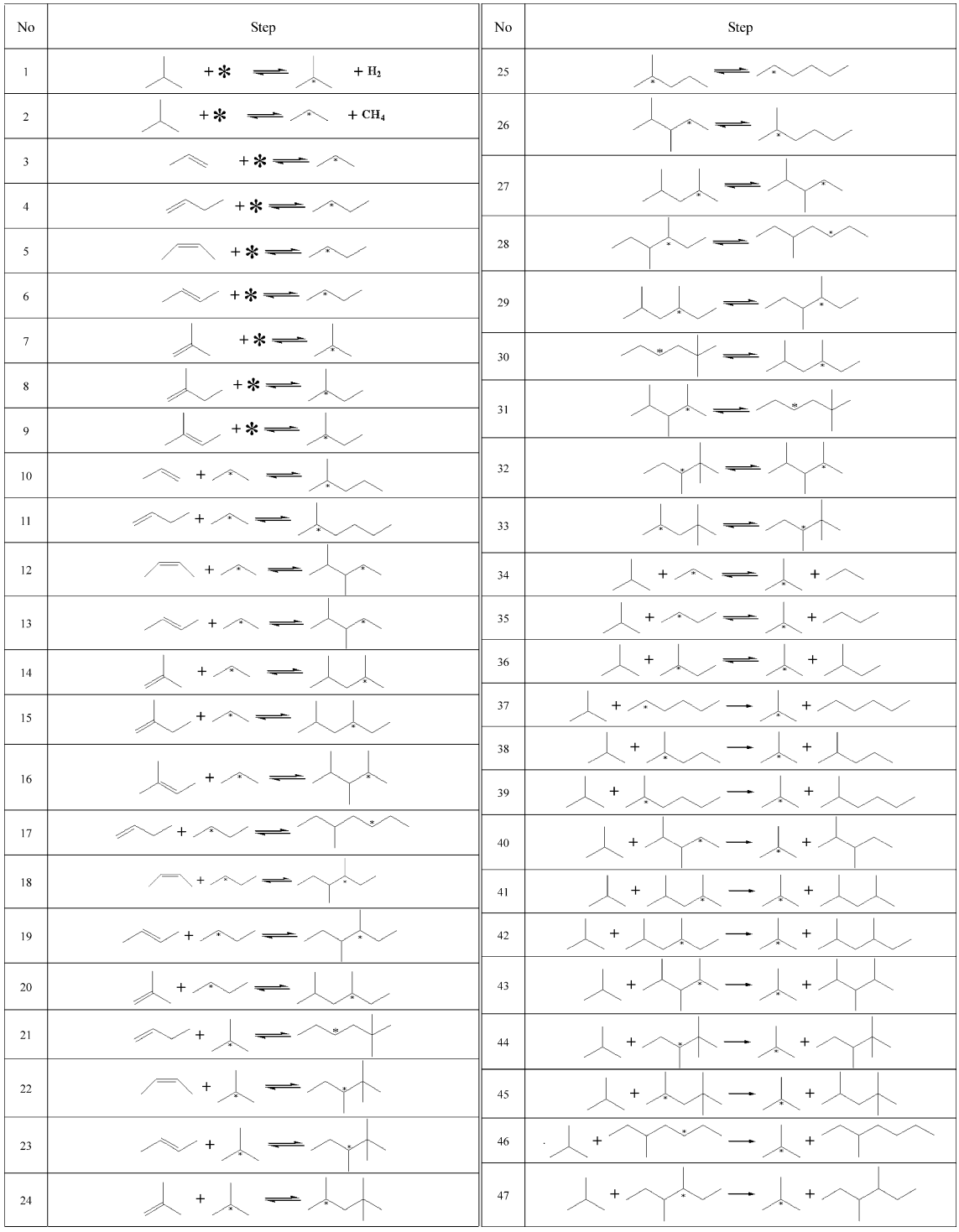

Fig. 7. Simplified reaction scheme for isobutane conversion over H-mordenite and β-zeolite catalysts.

from β-scission to hydride transfer. Fig. 9 shows that the net rates of β-scission and hydride transfer are similar to each other, and they are higher over β-zeolite compared to USY for all reaction conditions. At 473 K, the rate of monomolecular activation over USY is smaller by as much as 5 orders of magnitude than the rates of β-scission and hydride transfer. However, at 573 K, and 80% of isobutane, this difference narrows significantly; below 50 ppm of isobutylene in the feed, the rate of monomolecular activation becomes only 1 order of magnitude smaller than the rates of β-scission and hydride transfer.

Fig. 8 shows that $\sum |X_{\mathrm{RC},i}|$ for the monomolecular activation steps over β-zeolite are negligible at 473, particularly at 20% isobutane feed concentrations. However, at

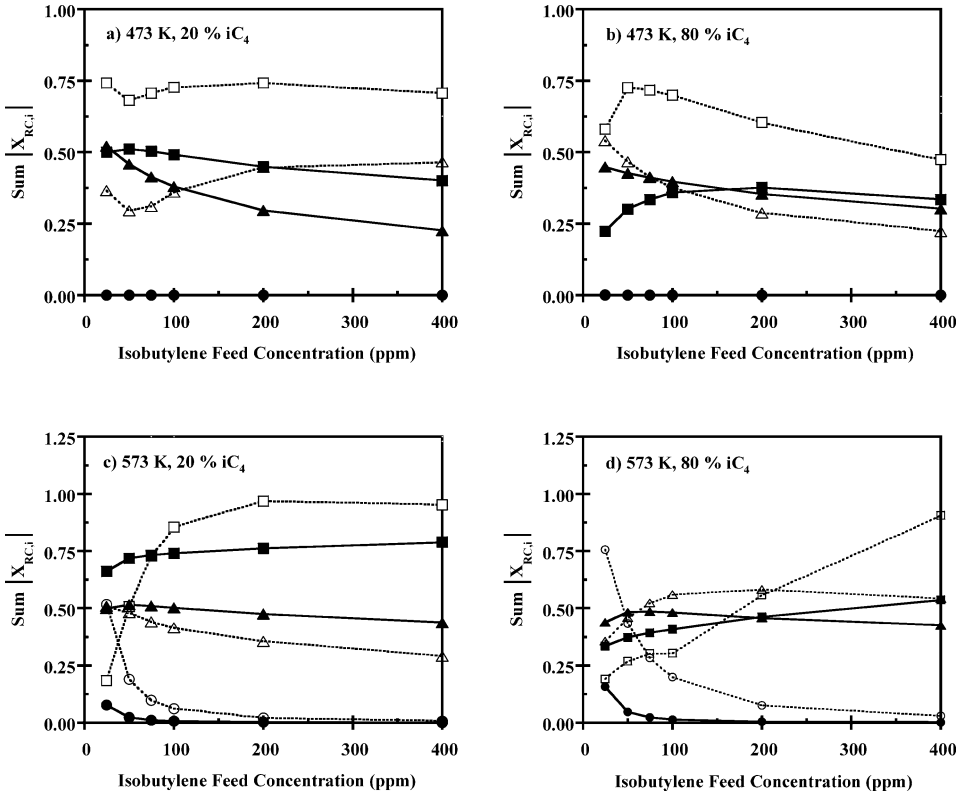

Fig. 8. Sum of the absolute values of $X_{\mathrm{RC},i}$ as a function of isobutylene feed concentration over USY (full symbols, solid lines) and β-zeolite (open symbols, dotted lines). Symbols: (○) sum of initiation steps, (□) sum of hydride transfer steps, (△) sum of oligomerization/β-scission steps.

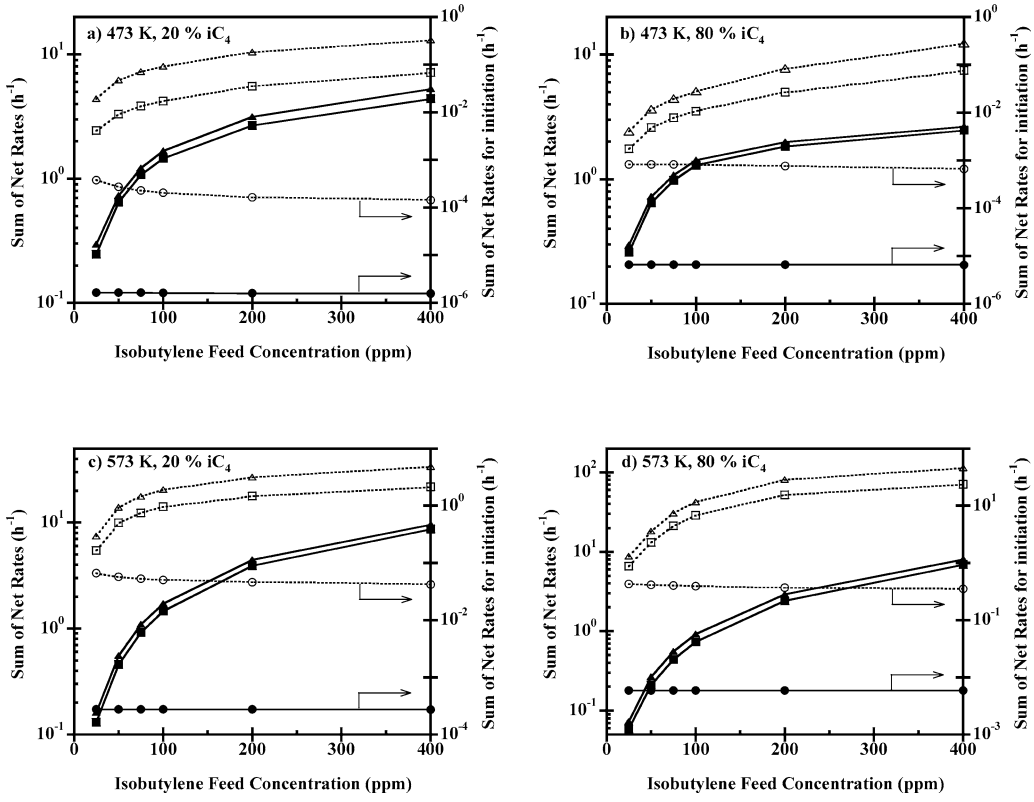

Fig. 9. Sum of the net rates as a function of isobutylene inlet concentration over USY (full symbol, solid line) and β-zeolite (open symbol, dotted line). Symbols: (○) sum of initiation steps, (□) sum of hydride transfer steps, (△) sum of oligomerization/β-scission steps.

573 K, $\sum|X_{\mathrm{RC},i}|$ for monomolecular activation becomes significant for a feed containing less than 100 and 200 ppm of isobutylene, for isobutane feed concentrations of 20 and 80%, respectively. For hydride transfer and β-scission steps over β-zeolite, temperature plays an important role. At 473 K, $\sum|X_{\mathrm{RC},i}|$ for hydride transfer is higher than for β-scission over the whole range of isobutylene and isobutane feed concentrations. As we increase the reaction temperature to 573 K in experiments with 20% isobutane, $\sum|X_{\mathrm{RC},i}|$ for monomolecular activation and β-scission steps become equally dominant for feeds containing less than 50 ppm of isobutylene, and the $\sum|X_{\mathrm{RC},i}|$ for hydride transfer is dominant for higher isobutylene feed concentrations. For experiments with 80% isobutane in the feed, the dominant $\sum|X_{\mathrm{RC},i}|$ is also a function of isobutylene feed concentration. As this concentration increases, $\sum|X_{\mathrm{RC},i}|$ for hydride transfer steps become progressively dominant. Fig. 9 indicates that, similar to USY, β-scission over β-zeolite shows the highest sum of net rates under all reaction conditions used. At 473 K, the net rate of monomolecular activation is smaller than the rates of other processes by ca. 4 orders of magnitude. This difference decreases to about 1 order of magnitude at 573 K, 80% of isobutane, and below 50 ppm of isobutylene in the feed. Importantly, the higher rate for β-scission over β-zeolite and H-mordenite, and to a lesser extent over USY, suggests the existence of more than one β-scission cycle per cycle of the other steps.

Our simulations indicate that the relative dominance of $\sum|X_{\mathrm{RC},i}|$ for hydride transfer over β-scission is higher for β-zeolite and H-mordenite than for USY. In addition, the differences between the net rates of β-scission and hydride transfer steps of β-zeolite and H-mordenite are always larger than for USY. These differences in the relative net rates of hydride transfer and β-scission steps account for differences observed in catalyst selectivity. One important difference we observe is that H-mordenite and β-zeolite give much higher paraffin/olefin ratios than USY. We discuss this in detail below.

Consider, for example, the formation of a paraffin C_n from the corresponding olefin, $C_n^=$. The gaseous olefin is in quasiequilibrium with the corresponding adsorbed alkoxy species, C_n*,

$$C_n^= + * \overset{K_{\mathrm{eq},n}}{\rightleftarrows} C_n*, \tag{6}$$

where $K_{\mathrm{eq},n}$ is the equilibrium constant. The adsorbed C_n* species undergoes hydride transfer with isobutane to give the corresponding paraffin plus an adsorbed isobutyl species,

$$iC_4 + C_n* \overset{k_{\mathrm{H}}}{\rightarrow} C_n + iC_4*, \tag{7}$$

where k_{H} is the rate constant. This step is shown as being irreversible because the pressure of the paraffin C_n is much lower than that of isobutane under our experimental conditions. The rate of formation of the paraffin, $\bar{r}_{C_n}$, is therefore equal to

$$\bar{r}_{C_n} = k_{\mathrm{H}} K_{\mathrm{eq},n} P_{iC_4} P_{C_n^=}(*), \tag{8}$$

where $(*)$ is the concentration of active sites. The turnover frequency, r_{C_n}, in the limit of low coverage is therefore

$$r_{C_n} = k_{\mathrm{H}} K_{\mathrm{eq},n} P_{iC_4} P_{C_n^=}. \tag{9}$$

The partial pressure of the product paraffin, P_{C_n}, may be calculated from the rate of formation of the paraffin by the expression

$$r_{C_n} = \frac{P_{C_n}}{P_{\mathrm{total}}} F_{\mathrm{total}}, \tag{10}$$

where P_{total} is the total pressure (1 atm), F_{total} is the total gaseous flow rate expressed as molecules per site per second (s^{-1}), and the rate, r_{C_n}, is a turnover frequency. From Eqs. (9) and (10), the paraffin/olefin ratio is given by

$$\frac{P_{C_n}}{P_{C_n^=}} = \frac{k_{\mathrm{H}} K_{\mathrm{eq},n} P_{iC_4}}{F_{\mathrm{total}}}. \tag{11}$$

According to transition state theory, k_{H} may be expressed as a quasiequilibrium between the reactants of the step (7) and the transition state for hydride transfer, $HT^\dagger$, as given by

$$iC_4 + C_n* \overset{K_{\mathrm{H}}^\dagger}{\rightleftarrows} HT^\dagger, \tag{12}$$

with an equilibrium constant $K_{\mathrm{H}}^\dagger$. The rate constant k_{H} is equal to the product of $K_{\mathrm{H}}^\dagger$ and a frequency factor, $\upsilon^\dagger$, and Eq. (11) may be written as

$$\frac{P_{C_n}}{P_{C_n^=}} = \frac{\upsilon^\dagger K_{\mathrm{H}}^\dagger K_{\mathrm{eq},n} P_{iC_4}}{F_{\mathrm{total}}}. \tag{13}$$

Thus, the paraffin/olefin ratio is controlled by the gas flow rate per acid site, F_{total}, and the value of $K_{\mathrm{H}}^\dagger K_{\mathrm{eq},n}$. For the more active β-zeolite and H-mordenite, F_{total} will be higher than for USY to obtain the same conversion. Hence for β-zeolite and H-mordenite, the higher F_{total} will make the ratio in Eq. (13) lower. However, this effect is more than compensated by the term $K_{\mathrm{H}}^\dagger K_{\mathrm{eq},n}$ which corresponds to an equilibrium constant for the following combined step:

$$iC_4 + C_n^= + * \overset{K^\dagger K_{\mathrm{eq},n}}{\rightleftarrows} HT^\dagger. \tag{14}$$

Importantly, the temperature dependence of the term $K_{\mathrm{H}}^\dagger \times K_{\mathrm{eq},n}$ is controlled by the energy of the transition state relative to the reactants in the gas phase, i.e., the composite activation energy barrier as defined earlier. The high paraffin/olefin ratios observed over H-mordenite and β-zeolite are thus primarily due to the lower values of the composite activation energy barriers for hydride transfer (by about 20–30 kJ mol^{-1}) over these zeolites compared to USY.

6. Concluding remarks

We have successfully extended our kinetic model previously developed for the conversion of isobutane over USY to describe reaction kinetics data over H-mordenite and β-zeolite under conditions where the reaction is initiated primarily by the addition of isobutylene to the feed, though

monomolecular activation steps become important at lower temperatures for these two catalysts than for USY. Composite activation energies, defined in terms of the energies of transition states relative to gas-phase reactants, control catalyst performance for isobutane conversion. The higher catalytic activity of H-mordenite and β-zeolite with respect to that of USY is due to lower composite activation energies for monomolecular activation steps as well as for hydride transfer and oligomerization/β-scission. The composite activation energies of monomolecular activation steps are lower by about 20–25 kJ mol^{-1} over H-mordenite and β-zeolite compared to USY, and this difference matches the differences in the heats of adsorption of alkanes on these zeolites obtained via calorimetric measurements [30,49].

Importantly, the composite activation energies of hydride transfer and β-scission/oligomerization steps are lower by about 20–30 kJ mol^{-1} over H-mordenite and β-zeolite compared to USY. We conclude that the same interactions responsible for stabilizing the transition states for monomolecular activation over zeolites are also important in stabilizing the transition states for the other reactions. Furthermore the heats of adsorption of olefins are more exothermic on H-mordenite and β-zeolite compared to USY, again indicating that the same interactions responsible for stabilizing the transition states for all monomolecular and bimolecular reactions are also important in stabilizing the adsorbed surface alkoxy reaction intermediates. These zeolitic interactions that seem to be common to several critical steps may be van der Waals forces engendered by the shape, nature, size, and chemical composition of the zeolite walls and cavities. These forces may stabilize transition states and influence the adsorption–desorption equilibrium and surface coverage, with or without directly influencing the active Brønsted acid site.

The differences observed in the performance of H-mordenite and β-zeolite for isobutane conversion versus the behavior of USY are probed more quantitatively using sensitivity analyses. The degree of rate control analyses shows the larger dominance of hydride transfer over β-scission for H-mordenite and β-zeolite compared to USY, with the net rates and the difference in net rates for these reactions being significantly larger for H-mordenite and β-zeolite. This difference accounts for the higher paraffin/olefin ratios observed in the products over H-mordenite and β-zeolite in terms of the lower composite activation energies for hydride transfer compared to that for USY.

Acknowledgments

We gratefully acknowledge the funding from the Department of Energy (Basic Energy Sciences) and Engelhard Corporation, which supported research at the University of Wisconsin. We thank Dr. Xinsheng Liu at Engelhard who carried out the FTIR studies.

References

[1] H. Hattori, O. Takahashi, M. Takagi, K. Tanabe, J. Catal. 68 (1981) 132.
[2] G.M. Kramer, G.B. McVicker, J.J. Ziemiak, J. Catal. 92 (1985) 355.
[3] W.O. Haag, R.M. Dessau, R.M. Lago, Stud. Surf. Sci. Catal. 60 (1991) 255.
[4] R. Shigeishi, A. Garfoth, I. Harris, J. Dwyer, J. Catal. 130 (1991) 423.
[5] H. Krannila, W.O. Haag, B. Gates, J. Catal. 135 (1992).
[6] M. Guisnet, N.S. Gnep, D. Aittaleb, Y.J. Doyomet, Appl. Catal. A 87 (1992) 255.
[7] Y. Zhao, G.R. Bamwenda, W.A. Groten, B.W. Wojciechowski, J. Catal. 140 (1993) 243.
[8] R.A. Asuquo, G. Eder-Mirth, J.A. Lercher, J. Catal. 155 (1995) 376.
[9] M. Guisnet, N.S. Gnep, Appl. Catal. A 146 (1996) 33.
[10] T.F. Narbeshuber, A. Brait, K. Seshan, J.A. Lercher, Appl. Catal. A 146 (1996) 119.
[11] T.F. Narbeshuber, M. Stockenhuber, A. Brait, K. Seshan, J.A. Lercher, J. Catal. 160 (1996) 183.
[12] K.B. Fogash, R.B. Larson, M.R. Gonzalez, J.M. Kobe, J.A. Dumesic, J. Catal. 163 (1996) 138.
[13] R.A. Asuquo, G. Eder-Mirth, K. Seshan, A.A.Z. Pieterse, J.A. Lercher, J. Catal. 168 (1997) 292.
[14] S.M. Babitz, M.A. Kuehne, H.H. Kung, Ind. Eng. Chem. Res. 36 (1997) 3027.
[15] G. Yaluris, R.J. Madon, J.A. Dumesic, J. Catal. 165 (1997) 205.
[16] R. Cortright, J.A. Dumesic, R.J. Madon, Top. Catal. 4 (1997) 15.
[17] A. Brait, A. Koopmans, H. Weinstabl, A. Ecker, K. Seshan, J.A. Lercher, Ind. Eng. Chem. Res. 37 (1998) 873.
[18] M.T. Tran, N.S. Gnep, G. Szabo, M. Guisnet, Appl. Catal. A 170 (1998) 49.
[19] Z. Hong, K.B. Fogash, R.M. Watwe, B. Kim, B.I. Masqueda-Jimenez, M.A. Natal-Santiago, J.M. Hill, J.A. Dumesic, J. Catal. 178 (1998) 489.
[20] S.M. Babitz, B.A. Williams, J.T. Miller, R.Q. Snurr, W.O. Haag, H.H. Kung, Appl. Catal. A 179 (1999) 71.
[21] Z. Hong, K.B. Fogash, J.A. Dumesic, Catal. Today 51 (1999) 269.
[22] B.A. Williams, S.M. Babitz, J.T. Miller, R.Q. Snurr, H.H. Kung, Appl. Catal. A 177 (1999) 161.
[23] H.H. Kung, B.A. Williams, S.M. Babitz, J.T. Miller, R.Q. Snurr, Catal. Today 52 (1999) 91.
[24] B.A. Williams, W. Ji, J.T. Miller, R.Q. Snurr, H.H. Kung, Appl. Catal. 203 (2000) 179.
[25] G.B. McVicker, G.M. Kramer, J.J. Ziemiak, J. Catal. 83 (1983) 286.
[26] G. Yaluris, J.E. Rekoske, L.M. Aparicio, R.J. Madon, J.A. Dumesic, J. Catal. 153 (1995) 54.
[27] G. Yaluris, J.E. Rekoske, L.M. Aparicio, R.J. Madon, J.A. Dumesic, J. Catal. 153 (1995) 65.
[28] A. Corma, P.J. Miguel, A.V. Orchillés, Ind. Eng. Chem. Res. 36 (1997) 3400.
[29] M.A. Sanchez-Castillo, N. Agarwal, C. Miller, R.D. Cortright, R. Madon, J.A. Dumesic, J. Catal. 204 (2001).
[30] S. Kotrel, M.P. Rosynek, J.H. Lunsford, J. Phys. Chem. B 103 (1999) 818.
[31] T.F. Narbeshuber, H. Vinek, J.A. Lercher, J. Catal. 157 (1995) 388.
[32] N. Agarwal, M.A. Sanchez-Castillo, R.D. Cortright, R.J. Madon, J.A. Dumesic, Ind. Eng. Chem. Res. 41 (2002) 4016.
[33] X. Liu, R.E. Truitt, G.D. Hodge, J. Catal. 176 (1998) 52.
[34] K.B. Fogash, Z. Hong, J.A. Dumesic, J. Catal. 173 (1998) 519.
[35] J. Engelhardt, J. Catal. 164 (1996) 449.
[36] J. Engelhardt, J. Valyon, J. Catal. 181 (1999) 294.
[37] E.A. Lombardo, W.K. Hall, J. Catal. 112 (1988) 565.
[38] J. Engelhardt, W.K. Hall, J. Catal. 125 (1990) 472.
[39] C. Stefanadis, B.C. Gates, W.O. Haag, J. Mol. Catal. 67 (1991) 363.

[40] P.V. Shertukde, G. Marcelin, G.A. Sill, W.K. Hall, J. Catal. 136 (1992) 446.
[41] J.E. Rekoske, R.J. Madon, L.M. Aparicio, J.A. Dumesic, Stud. Surf. Sci. Catal. 75 (1993) 1653.
[42] A. Corma, P.J. Miguel, A.V. Orchillés, J. Catal. 145 (1994) 171.
[43] W.O. Haag, R.M. Dessau, in: Proceedings 8th Int. Congr. Catal., Vol 2, Chemie, Berlin, 1984, p. II305, preprints, Fed. Rep. Ger.
[44] S.W. Benson, Thermochemical Kinetics, Wiley, New York, 1968.
[45] S.W. Benson, J.H. Buss, J. Chem. Phys. 29 (1969) 546.
[46] S.W. Benson, F.R. Cruickshank, D.M. Golden, G.R. Haugen, H.E. O'Neal, A.S. Rodgers, R. Shaw, R. Walsh, Chem. Rev. 69 (1969) 279.
[47] R.C. Reid, J.M. Prausnitz, B.E. Poling, The Properties of Gases and Liquids, McGraw–Hill, New York, 1987.
[48] F. Eder, M. Stockenhuber, J.A. Lercher, J. Phys. Chem. B 101 (1997) 5414.
[49] J.F. Denayer, G. Baron, J. Martens, P. Jacobs, J. Phys. Chem. B 102 (1998) 3077.
[50] V.B. Kazansky, M.V. Frash, R.A. van Santen, Appl. Catal. A 146 (1996) 225.
[51] A.M. Rigby, G.J. Kramer, R.A. van Santen, J. Catal. 170 (1997) 1.
[52] A. van de Runstraat, J.V. Grondelle, R.A. van Santen, Ind. Eng. Chem. Res. 36 (1997) 3116.
[53] W.E. Stewart, M.C. Caracotsios, Athena Visual Workbench, Stewart & Associates Engineering Software, Inc., Madison, 2000.
[54] C.T. Campbell, Top. Catal. 1 (1994) 353.
[55] R.D. Cortright, J.A. Dumesic, Adv. Catal. 46 (2001) 161.